

Received March 10, 2025; accepted June 27, 2025; Date of publication August 26, 2025.

The review of this paper was arranged by Associate Editor Fernanda de M. Carnielutti and Editor-in-Chief Heverton A. Pereira.

Digital Object Identifier <http://doi.org/10.18618/REP.e202549>

Introducing INEP PVSIm: A Free Offline Application to Assess the Effects of Parameter Variations on the I-V Curves of Photovoltaic Modules

Matheus M. da Silva¹, Victor F. Gruner¹, Thiago F. Rech^{1,*}, Tailan Orlando¹,
Kevin R. Costa², Jens Friebe², André L. Kirsten¹, Roberto F. Coelho¹

¹Federal University of Santa Catarina, Power Electronics Institute, Florianópolis – SC, Brazil.

²University of Kassel, Department of Power Electronics, Kassel, Germany

e-mail: matheusmms.eel@gmail.com; victorgruner@gmail.com; thiagofrech@hotmail.com*; tailan_orlando@hotmail.com, kevin.costa@uni-kassel.de, friebe@uni-kassel.de, kirsten.andre@ufsc.br; roberto@inep.ufsc.br.

*Corresponding author.

ABSTRACT This paper introduces INEP PVSIm, an offline application designed for teachers, students, and engineers to evaluate the behavior of photovoltaic (PV) modules. The application features a user-friendly interface that allows the simulation of I–V and P–V curves under different climate conditions, enabling real-time modification of parameters such as solar irradiance and temperature across a much broader range than typically provided in manufacturer datasheets. INEP PVSIm is developed as free Python-based code and offers significant educational potential in the field of Power Electronics, as analyzing the impact of parameter variations on PV generation is often a challenging task with direct implications for power converter design. In addition to presenting the application, this paper also formalizes, in a single document, the equations and methods adopted for the implementation of the one-diode model, providing an accessible yet accurate platform for both learning and practical analysis.

KEYWORDS Photovoltaic energy, One-diode model, Python, Education, I-V and I-V curves.

I. INTRODUCTION

In recent years, photovoltaic (PV) generators have emerged as one of the leading sources of renewable energy, driven by advancements in power electronics and simulation tools that enable the design of optimized systems. The high penetration of photovoltaic generation in the power system is mainly motivated by the global effort to reduce carbon emissions and achieve sustainability targets, while also benefiting from its status as the most cost-effective solution in many applications [1].

Accurate modeling of PV modules, particularly through tools that simulate current-voltage (I-V) curves, plays a key role in understanding the impact of environmental and operational conditions on PV performance. Such tools provide valuable insights, not only for educational purposes but also for practical engineering applications, as they illustrate the real-world behavior of PV modules.

Beyond design and performance optimization, the analysis of I-V curves is an insightful tool for evaluating the health of photovoltaic modules under real operating conditions. Its shape and variations enable the identification of faults and aging effects that compromise system efficiency, allowing the diagnosis of issues such as increased series resistance, short-circuited bypass diodes, local shading, and potential-induced degradation. I-V curve tracers capture these characteristics throughout the module's lifespan, delivering critical data for predictive maintenance and monitoring of module integrity, as detailed in [2].

To effectively represent these characteristics in a manageable format, the one-diode model has become widely adopted. Known for its sufficient accuracy, this model can represent the electrical behavior of PV modules using a simple electrical circuit with solar irradiance and temperature as inputs [3], [4]. As a tool for engineers and researchers, it supports both practical applications and theoretical analyses of PV performance [4]. However, teaching the principles behind the one-diode model can be challenging due to the complexity of the parameters involved [5].

The development of models to predict the electrical behavior of PV power plants has a significant impact on the field of Power Electronics, as variations in PV generation is usually considered during the design of power converters. In Power Electronics, simulation tools have already been widely used in advancing the teaching and understanding of concepts. Early developments [6] laid the groundwork with interactive web-based seminars utilizing Java applets to demonstrate key principles, effectively engaging students and enhancing their comprehension of complex topics. Subsequent work [7], [8] refined these methods by introducing circuit simulators specifically designed for interdisciplinary education, enabling students from diverse engineering backgrounds to explore power electronics through simulation tools.

Similarly, as the complexity of PV systems grew, researchers sought more precise and computationally efficient methods to improve these models. In [9], an effective method for extracting parameters from I-V curves is proposed, which significantly enhanced the precision of

simulations. Meanwhile [10] and [11] introduced analytical approaches that further refined the model's accuracy while simplifying its practical application. These advances addressed one of the main challenges in PV simulation: the non-linearity of the one-diode model.

The non-linear nature of the equations in the one-diode model requires sophisticated numerical methods for their solution. In this context, the optimization techniques developed in [12] and [13] improve the fitting of I–V curves, ensuring that simulated data closely match real-world performance. By combining algorithms like Newton–Raphson with heuristic approaches, researchers have achieved more accurate and faster parameter estimation.

Moreover, recent studies have focused on incorporating environmental factors such as temperature and irradiance into PV modeling. For instance, [14] examined the effects of temporal and environmental variations on PV performance, further enhancing the practical utility of these models for real-world applications, while [15] applied hybrid numerical methods to achieve faster and more accurate simulations. In parallel, industry-standard simulators such as PVSyst [16] and SolarPro [17] have become widely adopted for designing and optimizing PV systems, enabling engineers to simulate performance under varying operating conditions. However, despite their effectiveness for professional use, these platforms are often complex and not ideally suited for educational purposes.

These limitations encouraged the development of INEP PVSIm, which addresses the gap between industry-level simulators and educational tools. While it does not aim to replace advanced design software like PVSyst, it offers a more accessible platform for students and engineers to grasp the fundamentals of PV module behavior. Featuring an intuitive interface and real-time simulation capabilities, it greatly enhances the learning experience by allowing users to examine the effects of parameters like irradiance and temperature on PV performance.

This paper not only advances the evolution of I-V and P-V curves simulation by introducing a tool that merges educational value with practical utility but also formalizes in a single document the equations and methods adopted to model the one-diode-model.

II. I-V CURVE AND MATHEMATICAL MODELING

The one-diode model allows the electric representation of a photovoltaic (PV) module by the circuit illustrated in FIGURE 1. In this circuit, I_{ph} is the photogenerated current, R_s is the series resistance that represents the electrical contact losses and R_p is the parallel resistance that models the leakage current losses of the PV module, whereas D is the diode that models the semiconductor properties. The quantities V_{pv} and I_{pv} are the output voltage and current, respectively.

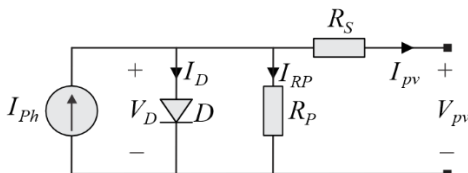


FIGURE 1. One-diode model that represents a photovoltaic module.

Evaluating the circuit by means of the Kirchhoff's laws, results in:

$$I_{pv} = I_{ph} - I_D - I_{RP}, \quad (1)$$

$$V_D = V_{pv} + R_s I_{pv}, \quad (2)$$

$$I_{RP} = \frac{V_D}{R_p} = \frac{V_{pv} + R_s I_{pv}}{R_p}. \quad (3)$$

From (1) it is noted that I_{pv} can be described as a function of I_{ph} , I_D , and I_{RP} . Since I_{RP} has already been defined in (3), only I_{ph} and I_D remain to be determined. The photogenerated current I_{ph} depends on the solar irradiance G and the temperature T to which the photovoltaic module is subjected, and can be represented by [4]:

$$I_{ph} = \frac{G}{G_{STC}} I_{ph}^{STC} [1 + \alpha(T - T^{STC})], \quad (4)$$

where the superscript term "STC" represents the parameter in question found at the datasheet under standard test conditions, and α is the thermal coefficient of I_{sc} provided in the PV module datasheet.

Additionally, the current I_D across the diode can be rigorously approximated by the Shockley equation [8]:

$$I_D = I_s \left(e^{\frac{qV_D}{AkT}} - 1 \right), \quad (5)$$

where $k = 1.38 \times 10^{-23}$ J/K and $q = 1.602 \times 10^{-19}$ C are the Boltzmann constant and the elementary charge, respectively, whereas A is the ideality factor of the diode and I_s is its saturation current. In practice, I_s is related to the thermal ionization at the pn junction and depends on the temperature T :

$$I_s = I_s^{STC} \left(\frac{T}{T^{STC}} \right)^3 e^{\frac{n_s q E_G}{Ak} \left(\frac{1}{T^{STC}} - \frac{1}{T} \right)}. \quad (6)$$

In (6), n_s is the number of cell connected in series that compose the PV module and E_G is the semiconductor gap energy, which can also be described as a function of the temperature T [9]:

$$E_G = E_{G0} - \frac{k_1 T^2}{T + k_2}, \quad (7)$$

where the coefficients $k_1 = 4.73 \times 10^{-4}$ eV/K, $k_2 = 636$ K, and $E_{G0} = 1.166$ eV are specific for silicon cells.

By substituting (7) into (6), and the obtained result in (5), it is possible to write the complete equation for I_D :

$$I_D = I_s^{STC} \left(\frac{T}{T^{STC}} \right)^3 \left(e^{\frac{q(R_s I_{pv} + V_{pv})}{AkT}} - 1 \right) e^{\frac{n_s q}{Ak} \left(E_{G0} - \frac{k_1 T^2}{T + k_2} \right) \left(\frac{1}{T^{STC}} - \frac{1}{T} \right)}. \quad (8)$$

Finally, substituting (3), (4) and (8) into (1), an equation to describe the relationship between I_{pv} and V_{pv} of the photovoltaic module can finally be derived:

$$I_{pv} = \frac{G}{G_{STC}} I_{ph}^{STC} [1 + \alpha(T - T^{STC})] - I_s^{STC} \left(\frac{T}{T^{STC}} \right)^3 \left(e^{\frac{q(R_s I_{pv} + V_{pv})}{AkT}} - 1 \right) e^{\frac{n_s q}{Ak} \left(E_{G0} - \frac{k_1 T^2}{T + k_2} \right) \left(\frac{1}{T^{STC}} - \frac{1}{T} \right)} - \frac{R_s I_{pv} + V_{pv}}{R_p}. \quad (9)$$

Equation (9) has five unknown variables: A , I_{ph}^{STC} , I_s^{STC} , R_s and R_p . Finding a correct solution for these parameters requires knowledge of five equations that relate to them. The

procedures for obtaining these five equations are explored in the next section.

III. SYSTEM OF EQUATIONS TO DETERMINE THE REMAINING FIVE PARAMETERS

To obtain the system of equations mentioned above, it is necessary to analyze the operation of the photovoltaic generator from different perspectives. First, let's assume that the PV generator is operating at the standard test conditions ($G = G^{STC}$ and $T = T^{STC}$), as these are the conditions under which the PV module is characterized in the datasheet. With this assumption, (9) can be simplified as:

$$I_{pv} = I_{Ph}^{STC} - I_s^{STC} \left(e^{\frac{q(R_s I_{pv} + V_{pv})}{AkT^{STC}}} - 1 \right) - \frac{R_s I_{pv} + V_{pv}}{R_p}. \quad (10)$$

Three operating points of the I-V curve under standard test conditions are provided in the PV module datasheets. From these three operating points, three of the five required equations can be obtained to describe the module operation at the short-circuit, open-circuit, and maximum power point conditions.

In short-circuit operation, the voltage V_{pv} measured between the PV module terminals is null, and the current I_{pv} is the short-circuit current I_{sc}^{STC} . In open circuit operation, the voltage V_{pv} is the open-circuit voltage V_{oc}^{STC} , while the current I_{pv} is equal to zero. Finally, at the maximum power point, the voltage V_{pv} and the current I_{pv} assume the values V_{mp}^{STC} and I_{mp}^{STC} , respectively. The substitution of these operating points, one by one, into (10), allows writing:

$$I_{Ph}^{STC} - I_s^{STC} \left(e^{\frac{qR_s I_{sc}^{STC}}{AkT^{STC}}} - 1 \right) - \frac{R_s I_{sc}^{STC}}{R_p} = 0, \quad (11)$$

$$I_{Ph}^{STC} - I_s^{STC} \left(e^{\frac{qV_{oc}^{STC}}{AkT^{STC}}} - 1 \right) - \frac{V_{oc}^{STC}}{R_p} = 0, \quad (12)$$

$$I_{Ph}^{STC} - I_s^{STC} \left(e^{\frac{qR_s I_{mp}^{STC}}{AkT^{STC}}} - 1 \right) - \frac{R_s I_{mp}^{STC} + V_{mp}^{STC}}{R_p} - I_{mp}^{STC} = 0. \quad (13)$$

The fourth equation is obtained by inspecting the P-V curve, which reveals that the derivative of the PV output power in respect with the voltage is null at the maximum power point, as shown in FIGURE 2. Therefore, using the Fermat's Theorem on Local Extrema, we can obtain an equation to describe this condition:

$$\left. \frac{dP_{pv}}{dV_{pv}} \right|_{V_{pv}=V_{mp}^{STC}} = 0. \quad (14)$$

Now, using the relation $P_{pv} = V_{pv} I_{pv}$ and knowing that I_{pv} is defined in (10), it is possible to write:

$$\frac{dP_{pv}}{dV_{pv}} = \frac{d}{dV_{pv}} \left[V_{pv} - V_{pv} I_s^{STC} \left(e^{\frac{q(R_s I_{pv} + V_{pv})}{AkT^{STC}}} \right) - \frac{R_s V_{pv} I_{pv} + V_{pv}^2}{R_p} \right]. \quad (15)$$

To solve this last equation, it must be considered that the current I_{pv} is not constant in respect to the variations of V_{pv} . With this information, we apply the relation $I_{pv} = P_{pv} / V_{pv}$ in (15) to solve the derivative implicitly, obtaining:

$$\frac{dP_{pv}}{dV_{pv}} = \frac{I_{Ph}^{STC} - \frac{2V_{pv}}{R_p} + I_s^{STC} - I_s^{STC} \left[1 + \frac{q(V_{pv} - R_s I_{pv})}{AkT^{STC}} \right] e^{\frac{q(R_s I_{pv} + V_{pv})}{AkT^{STC}}}}{1 + \frac{R_s}{R_p} + \frac{qR_s I_{Ph}^{STC}}{AkT^{STC}} e^{\frac{q(R_s I_{pv} + V_{pv})}{AkT^{STC}}}}. \quad (16)$$

In addition, we apply the constraints of (14) into (16) to find the fourth equation of the system:

$$I_{Ph}^{STC} - \frac{2V_{mp}^{STC}}{R_p} + I_s^{STC} - I_s^{STC} \left[1 + \frac{q(V_{mp}^{STC} - R_s I_{mp}^{STC})}{AkT^{STC}} \right] e^{\frac{q(R_s I_{mp}^{STC} + V_{mp}^{STC})}{AkT^{STC}}} = 0. \quad (17)$$

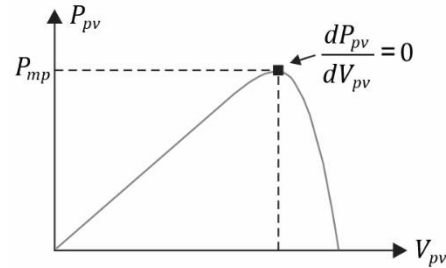


FIGURE 2. P-V curve with indication of the maximum power point.

Finally, the fifth equation is obtained by inspecting the I-V curve of FIGURE 3, which evidence that the derivative of the PV output current in respect with the output voltage, at the short-circuit operating point, is negative and inversely proportional to R_p .

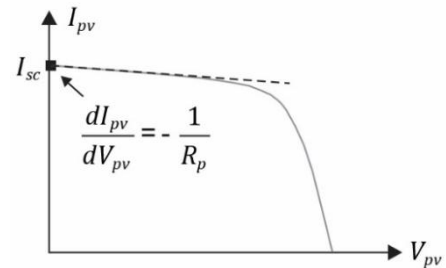


FIGURE 3. I-V curve with indication of the short-circuit operating point.

This last equation can be derived by the analysis of the one-diode model at the short-circuit condition, as presented in FIGURE 4.

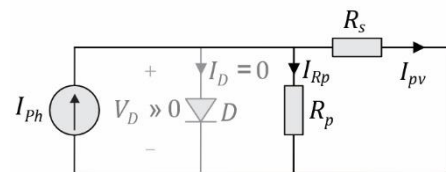


FIGURE 4. One-diode model at short-circuit condition.

As can be observed, the voltage on the diode is equal to the voltage drop across the resistor R_s ($V_D = R_s I_s$). Since R_s is in the order of milliohms, V_D is too reduced to bias the diode, which remains blocked. Therefore, around the short-circuit operating point, the slope of the I-V curve is majorly caused by the leakage current flowing through the parallel resistor R_p . As a result, it is possible to conclude that the rate of variation of the current I_{pv} in relation to the photogenerated voltage V_{pv} is given by:

$$\left. \frac{dI_{pv}}{dV_{pv}} \right|_{V_{pv}=0, I_{pv}=I_{sc}^{STC}} = -\frac{1}{R_p}. \quad (18)$$

To obtain the derivative of I_{pv} with respect to V_{pv} , we use (10), such that:

$$\frac{dI_{pv}}{dV_{pv}} = \frac{d}{dV_{pv}} \left[I_{Ph}^{STC} - I_s^{STC} \left(e^{\frac{q(R_s I_{pv} + V_{pv})}{A k T^{STC}}} - 1 \right) - \frac{R_s I_{pv} + V_{pv}}{R_p} \right]. \quad (19)$$

Again, using implicit derivation and applying the restrictions of (18), it is possible to obtain the fifth and final equation:

$$R_s + \frac{q I_s^{STC} R_p (R_s - R_p)}{A k T^{STC}} e^{\frac{q I_s^{STC}}{A k T^{STC}}} = 0. \quad (20)$$

Finally, (11), (12), (13), (17) and (20) may be grouped in a system of equations whose solution leads to the five unknown parameters: A , I_{Ph}^{STC} , I_s^{STC} , R_s and R_p :

$$\begin{cases} I_{Ph}^{STC} - I_s^{STC} \left(e^{\frac{q R_s I_s^{STC}}{A k T^{STC}}} - 1 \right) - \frac{R_s I_s^{STC}}{R_p} - I_{sc}^{STC} = 0, \\ I_{Ph}^{STC} - I_s^{STC} \left(e^{\frac{q V_{oc}^{STC}}{A k T^{STC}}} - 1 \right) - \frac{V_{oc}^{STC}}{R_p} = 0, \\ I_{Ph}^{STC} - I_s^{STC} \left(e^{\frac{q(R_s I_{mp}^{STC} + V_{mp}^{STC})}{A k T^{STC}}} - 1 \right) - \frac{R_s I_{mp}^{STC} + V_{mp}^{STC}}{R_p} - I_{mp}^{STC} = 0, \\ I_{Ph}^{STC} - \frac{2V_{mp}^{STC}}{R_p} + I_s^{STC} - I_s^{STC} \left[1 + \frac{q(V_{mp}^{STC} - R_s I_{mp}^{STC})}{A k T^{STC}} \right] e^{\frac{q(R_s I_{mp}^{STC} + V_{mp}^{STC})}{A k T^{STC}}} = 0 \\ R_s + \frac{q I_s^{STC} R_p (R_s - R_p)}{A k T^{STC}} e^{\frac{q I_s^{STC}}{A k T^{STC}}} = 0. \end{cases}$$

As can be noted from the presented system, the equations are non-linear, so it is necessary to use numerical methods to solve them. To run these numerical methods, proper initial values need to be assigned to the unknown variables, so that the convergence is achieved with a smaller number of iterations. To obtain the initial values of the series and parallel resistances, the I-V curve may be approximated by means of two straight-line segments, as shown in FIGURE 5.

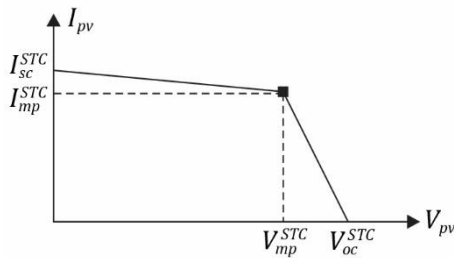


FIGURE 5. Approximation of the I-V curve by means of straight-line segments to determine the initial values of R_s and R_p .

Considering that the slope of the straight line to the left of the maximum power point is caused by the leakage current through R_p , and that the slope of the straight line to the right of the maximum power point is caused by the voltage drop in R_s , one can write:

$$R_{s0} = \frac{V_{oc}^{STC} - V_{mp}^{STC}}{I_{mp}^{STC}}, \quad (21)$$

$$R_{p0} = \frac{V_{mp}^{STC}}{I_{sc}^{STC} - I_{mp}^{STC}}. \quad (22)$$

Additionally, the initial value of the photogenerated current I_{Ph0}^{STC} can be approximated by the short-circuit current

itself, since in the short-circuit condition shown in FIGURE 4, the diode is reversely biased and the current flowing through R_p can be neglected. Thus:

$$I_{Ph0}^{STC} = I_{sc}^{STC}. \quad (23)$$

The next initial condition is the emission coefficient A . This coefficient is dimensionless and ranges from 1 to 2 to each solar cell. Therefore, considering that a PV module is composed by n_s cells associated in series, it is fair to infer that $n_s < A < 2n_s$. For simplicity, the lower limit is adopted:

$$A_0 = n_s. \quad (24)$$

Finally, we can approximate the value of I_s^{STC} on the scale of nanoamperes, since this is the typical magnitude of the reverse saturation current of silicon junction diodes. In light of this, it is assumed that:

$$I_{s0}^{STC} = 1 \text{ nA}. \quad (25)$$

A. MODEL VALIDATION

After determining the initial values of the quantities related to the model, an iterative method can be employed to solve the system of equations and obtain their final values. The study of algorithms for the numerical solution of non-linear systems is not within the scope of this paper. A script developed by using Python software was used for obtaining preliminary results. Based on this script, the five parameters of predefined photovoltaic modules with 36, 60, and 72 cells connected in series were determined and are shown in TABLE I.

TABLE I. Predefined modules parameters.

Parameter	VE136PV [18]	TSM-PC05A [19]	HiS-S350TI [20]
P_{mp}	150 W	250 W	350 W
n_s	36 cells	60 cells	72 cells
I_{Ph}^{STC}	8.841 A	8.790 A	9.601 A
I_s^{STC}	88.35 nA	2.040 nA	31.73 nA
A	47.67	66.67	93.89
R_s	109.6 mΩ	343.8 mΩ	183.9 mΩ
R_p	830 Ω	7.032 kΩ	2.59 kΩ

Now it is possible to replace the parameters of TABLE I in equation (9) and plot the I-V curve of the respective module (or the array) for different values of solar irradiance and temperature. As preliminary results, Figure 6 presents the I-V curves for the three modules whose parameters are summarized in TABLE I. Readers are encouraged to verify the validity of the models by comparing the curves in FIGURE 6 with those found in the respective PV module's datasheet and confirm that the errors are negligible.

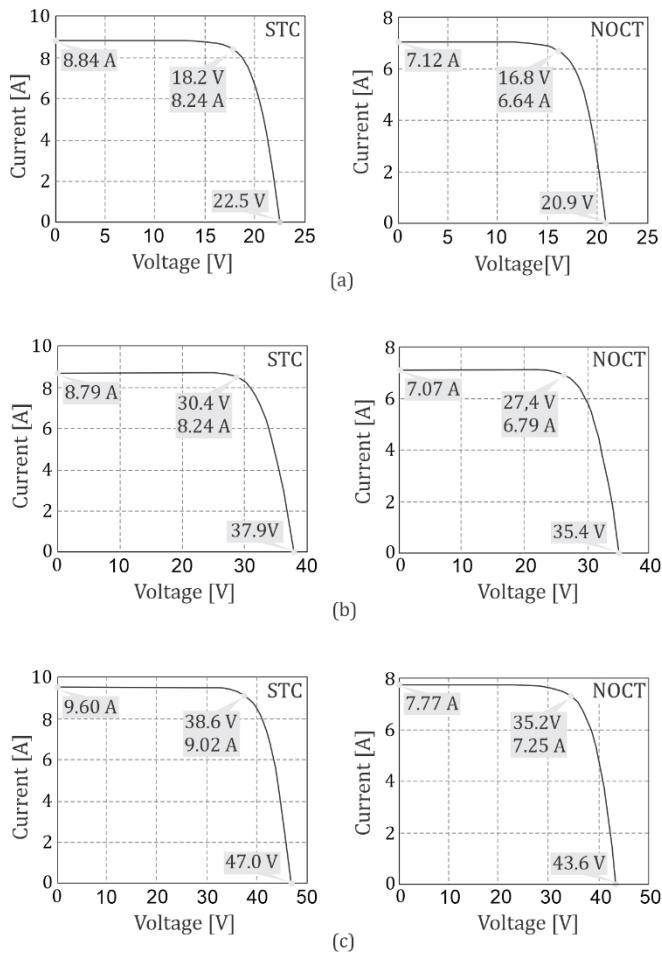


FIGURE 6. I-V curves obtained under standard test conditions (STC) and nominal operating cell temperature (NOCT) conditions for the predefined photovoltaic modules described in TABLE I: (a) VE-136PV; (b) TSM-PC05A; (c) HiS-S350TI.

B. APPLICATION DEVELOPMENT

The application focus of this paper was developed using the Python programming language in conjunction with libraries that were helpful in the process. As a base, the Tkinter library was used to shape the application, its windows, and buttons.

To solve the system of equations, an algorithm written in the Python programming language was used. To use this algorithm, and the Python module "subprocess" were employed. With the help of these libraries, the main code can receive the results of the algorithm, which is processed.

For modeling the I-V curve, the presented equations are implemented in a recursive way, using loops iterating each point of the curve. The used iteration variable was the voltage in the module terminals, V_{pv} , which increases with a step of 0.1 V.

For each step, the current I_{pv} is calculated according to (10), until the value of V_{pv} becomes equivalent to the open-circuit voltage V_{oc} , at which point the current I_{pv} becomes zero and the loop ends. This results in the I-V curve plot of the module under evaluation. Through the I-V curve it is also possible to plot the P-V curve just multiplying each value of I_{pv} by the respective value of V_{pv} . For visualization purposes, the P-V curve is multiplied by a scale factor before being shown in the graph.

The Matplotlib library was used to plot the I-V curve, as well as the sliders that change parameters such as the

temperature (T) and solar irradiance (G). Dotted lines have also been drawn over V_{mp} and I_{mp} , which indicate the quantities of the module at the maximum power point. Similar lines have additionally been drawn over the I_{sc} and V_{oc} values.

Something important to note is that the module's open-circuit voltage V_{oc} and short-circuit current I_{sc} are sensitive to the operating temperature T , whereas I_{sc} also varies with the solar irradiance G . Therefore, when modifying G or T by means of the sliders, the following equations are employed to update the related output variables:

$$I_{sc} = \frac{G}{G_{STC}} I_{sc}^{STC} [1 + \alpha(T - T^{STC})], \quad (26)$$

$$V_{oc} = V_{oc}^{STC} [1 + \beta(T - T^{STC})], \quad (27)$$

where α and β are thermal coefficients of the short-circuit current and open-circuit voltage, respectively. They can be found on the photovoltaic module datasheet.

IV. RESULTS

The main result of this research is an easy-to-use application that can have a major impact on demonstrating the influence of climatic and structural parameters on photovoltaic generators in an intuitive way.

For comply with this objective, the application has a home screen named "PV Calculator". When clicking on "start" the users are introduced to the "Mode Selection" screen depicted in FIGURE 7, for where they can define whether they want to enter the parameters of a specific module or select an example module to have the curves plotted.

The "Predefined Modules" screen has some examples of predefined photovoltaic modules, which do not require any data to be entered in order to have their curves plotted, making it easier for a user who wants to inspect them quickly and test the application's functionality, as shown in FIGURE 8. The modules showcased on the "Predefined Modules" screen are the V-Energy VE136PV, Trina Solar TSM-PC05A and Hyundai HiS-S350TI, referenced in [5], which have the features described in TABLE I.

Additionally, the "Parameters" screen illustrated in FIGURE 9, allows the user setting the parameters input for plotting the curves of the desired photovoltaic module. In this case, the user only needs to enter the data found on the module's datasheet.

After entering the parameters or choosing the desired example module, the user has access to the I-V (in red) and P-V (in green) curves of the photovoltaic module, including the sliders for changing parameters and the indication of lines above the maximum power point, in accordance to FIGURE 10, where the x -axis is defined in volts (V) and the y -axis in amperes (A). As already mentioned, for visualization purposes the power is not on the original scale, so it is not appropriate to graphically measure its value along the curve. By changing the position of the sliders, the curves are adjusted in real time according to the applied change. An example of curve updated by the sliders is illustrated in FIGURE 11.

The flowchart for the curve's calculation is depicted in FIGURE 12. Initially, the interface requests and stores the parameters of the PV module provided from the user in

variables. After this, Python's subprocess modules are employed to solve the system of equations and return the calculated parameters to Python variables. With the parameters entered by the user and those calculated by the Python code, it is possible to proceed to the curve's calculation.

The equations that do not require any iterative process are calculated first, which are equations (4), (6) and (7). Subsequently, lists are created in which the current, voltage and power values will be stored to form the I-V and P-V curves. Next, the equations (2), (3), and (5), which require an iterative process, since the I_{pv} equation is recursive, are solved. The process starts with an iterative loop using the voltage V_{pv} as the iteration variable, which is incremented at each iteration by 0.1 V. Every iteration, the values of I_{pv} are calculated by (9), then I_{pv} , V_{pv} and P_{pv} values are stored to form the curves. The loop continues until the value of V_{pv} reaches the short-circuit voltage V_{oc} , at which point the curve is finalized. The plot of the list of points is accomplished using the Matplotlib library.

Once the loop is completed, the I-V and P-V curves are displayed on the screen and can be modified using sliders that adjust the parameters T , G , R_s , R_p , A , I_s , and I_{ph} , enabling real-time curve updates. When a slider is moved, the values of V_{oc} and I_{sc} are recalculated according to the modified parameter, and the code returns to the step where the non-iterative equations are evaluated. The iterative process is then repeated, updating the curves accordingly.



FIGURE 7. Main screens of the application: (a) image of the application “home screen”; (b) image of the application “mode selection” screen.

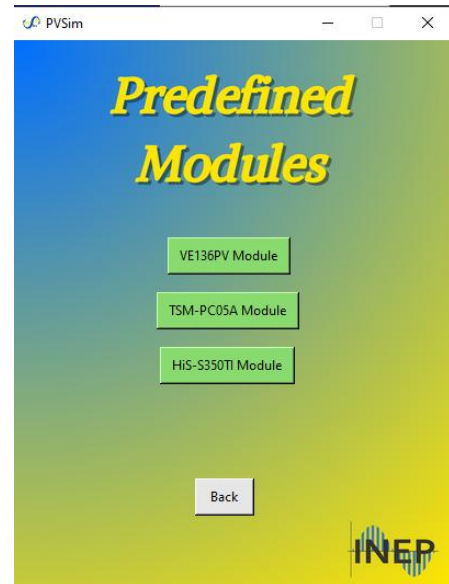


FIGURE 8. Image of the application “Predefined modules” screen.

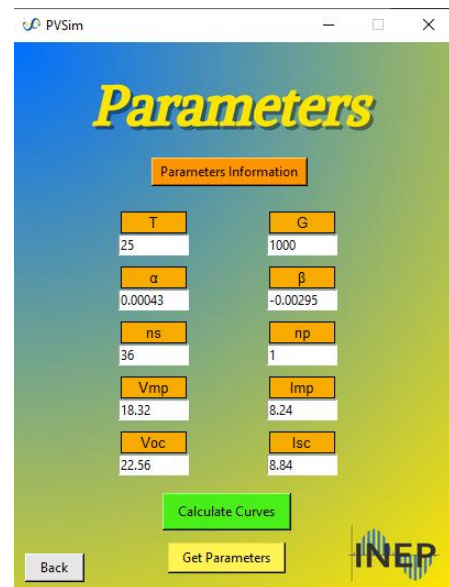


FIGURE 9. Image of the application “Parameters” screen.

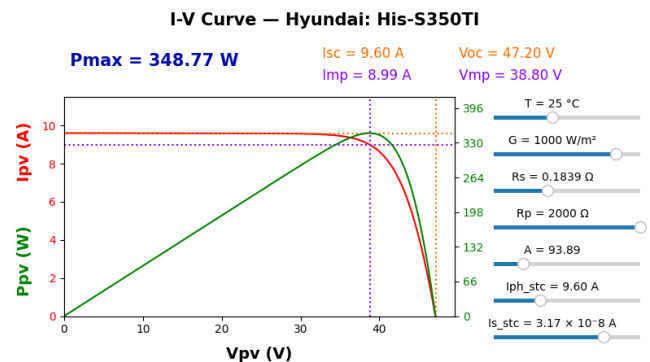


FIGURE 10. Image of the curves generated by the application.

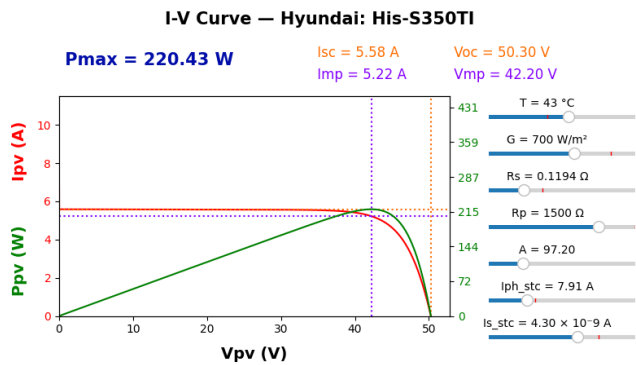


FIGURE 11. Image of the curves generated by the application, with modified sliders.

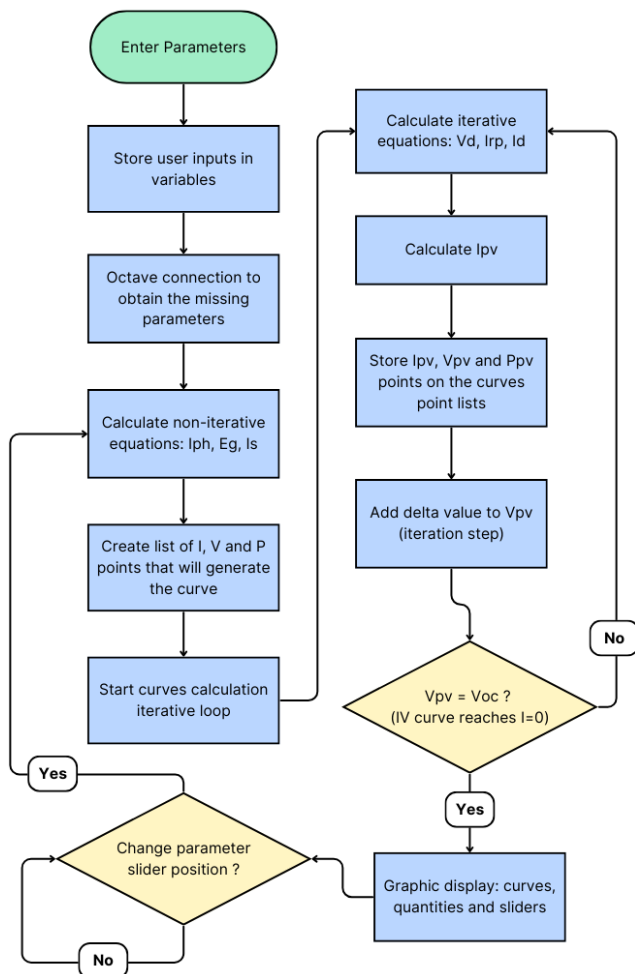


FIGURE 12. Flowchart of the algorithm used in the application.

V. CONCLUSION

This paper has introduced the INEP PVSIM, an offline application designed for teachers, students, and engineers to evaluate the behavior of photovoltaic (PV) modules. Through the developed application available for desktop, it is possible to intuitively analyze the influence of parameters T , G , R_s and R_p on the I-V and P-V curves of photovoltaic modules, requiring only the datasheet information entered by the user. This application has great potential to be applied in educational way, to demonstrate to the students how parametric and climatical variations affect photovoltaic generation curves.

In the future, the tool could be enhanced to include additional features related to the operation of photovoltaic modules, or to analyze the performance of the same module under different operating conditions. The application is freely available for download at:

<https://inep.ufsc.br/2025/06/04/inep-pvsim-a-free-offline-application-to-assess-the-effects-of-parameter-variations-on-the-i-v-curves-of-photovoltaic-modules/>.

ACKNOWLEDGMENT

The authors would like to thank the Coordination for the Improvement of Higher Education Personnel (CAPES) for the financial support provided to this project through the CAPES/DAAD – PROBRAL Program: Project number 8887.894991/2023-00. The authors are also grateful to acknowledge the support provided by the Tutorial Education program (PET) from the Brazilian Ministry of Education.

AUTHOR'S CONTRIBUTIONS

M.M.SILVA: Conceptualization, Data Curation, Funding Acquisition, Investigation, Methodology, Software, Validation, Visualization, Writing – Review & Editing. **T.F.RECH:** Project Administration, Software, Validation, Visualization, Writing – Original Draft, Writing – Review & Editing. **T.ORLANDO:** Writing – Original Draft, Writing – Review & Editing. **V.F.GRUNER:** Writing – Original Draft, Writing – Review & Editing. **J.FRIEBE:** Formal Analysis, Visualization, Writing – Original Draft. **K.R.COSTA:** Writing – Original Draft. **A.L.KIRSTEN:** Writing – Original Draft. **R.F.COELHO:** Conceptualization, Data Curation, Formal Analysis, Funding Acquisition, Project Administration, Resources, Supervision, Validation, Visualization, Writing – Original Draft, Writing – Review & Editing.

PLAGIARISM POLICY

This article was submitted to the similarity system provided by Crossref and powered by iThenticate – Similarity Check.

DATA AVAILABILITY

The data used in this research is available in the body of the document.

REFERENCES

- [1] REN21, "Renewables 2023 Global Status Report," *REN21 Secretariat*, 2023.
- [2] T. A. Pereira, L. Schmitz, W. M. dos Santos, D. C. Martins, and R. F. Coelho, "Design of a Portable Photovoltaic I-V Curve Tracer Based on the DC-DC Converter Method," *IEEE Journal of Photovoltaics*, vol. 11, no. 2, pp. 552-560, Mar. 2021. Doi: [10.1109/JPHOTOV.2021.3049903](https://doi.org/10.1109/JPHOTOV.2021.3049903)
- [3] T. Esram and P. L. Chapman, "Comparison of Photovoltaic Array Maximum Power Point Tracking Techniques," *IEEE Trans. Energy Convers.*, vol. 22, no. 2, pp. 439-449, Jun. 2007. Doi: [10.1109/TEC.2006.874230](https://doi.org/10.1109/TEC.2006.874230)
- [4] M. G. Villalva, J. R. Gazoli, and E. Ruppert Filho, "Comprehensive Approach to Modeling and Simulation of Photovoltaic Arrays," *IEEE Trans. Power Electron.*, vol. 24, no. 5, pp. 1198-1208, May 2009. Doi: [10.1109/TPEL.2009.2013862](https://doi.org/10.1109/TPEL.2009.2013862)
- [5] W. De Soto, S. A. Klein, and W. A. Beckman, "Improvement and Validation of a Model for Photovoltaic Array Performance," *Sol.*

- Energy*, vol. 80, no. 1, pp. 78-88, Jan. 2006. Doi: [10.1016/j.solener.2005.06.010](https://doi.org/10.1016/j.solener.2005.06.010)
- [6] U. Drofenik and J. W. Kolar, "Interactive Power Electronics Seminar (iPES) - A Web-Based Introductory Power Electronics Course Employing Java-Applets," in *Proc. IEEE Power Electron. Spec. Conf.*, 2002, pp. 443-448. Doi: [10.1109/PSEC.2002.1022493](https://doi.org/10.1109/PSEC.2002.1022493)
 - [7] E. Hiraki, M. Ishihara, and K. Umetani, "Introduction of Circuit Simulator to Power Electronics Education in Interdisciplinary Educational Environment," in *Proc. IEEE Int. Conf. E-Learning in Ind. Electron.*, 2023, pp. 1-5. Doi: [10.1109/ICELIE58531.2023.10313100](https://doi.org/10.1109/ICELIE58531.2023.10313100)
 - [8] A. Musing, U. Drofenik, and J. W. Kolar, "New circuit simulation applets for online education in power electronics," in *2011 5th IEEE International Conference on E-Learning in Industrial Electronics (ICELIE)*, Melbourne, Australia: IEEE, Nov. 2011, pp. 70-75. Doi: [10.1109/ICELIE.2011.6130028](https://doi.org/10.1109/ICELIE.2011.6130028)
 - [9] A. Laudani, F. R. Fulginei, and A. Salvani, "High Performing Extraction Procedure for the One-Diode Model of a Photovoltaic Panel from Experimental I-V Curves by Using Reduced Forms," *Sol. Energy*, vol. 103, pp. 316-326, 2014. Doi: [10.1016/j.solener.2014.02.014](https://doi.org/10.1016/j.solener.2014.02.014)
 - [10] H. Mokhliss, A. El-Amiri, and K. Rais, "Estimation of Five Parameters of Photovoltaic Modules Using a Synergetic Control Theory Approach," *J. Comput. Electron.*, vol. 18, no. 1, pp. 241-250, 2019. Doi: [10.1007/s10825-018-1253-2](https://doi.org/10.1007/s10825-018-1253-2)
 - [11] J. M. Alvarez, D. Alfonso-Corcuera, E. Roibas, J. Cubas, J. L. Cubero, A. G. Estrada, R. J. Puente, M. Sanabria, and S. Pindado, "Analytical Modeling of Current-Voltage Photovoltaic Performance: An Easy Approach to Solar Panel Behavior," *Appl. Sci.*, vol. 11, no. 9, 4250, 2021. Doi: [10.3390/app11094250](https://doi.org/10.3390/app11094250)
 - [12] H. M. Ridha, H. Hizam, S. Mirjalili, M. L. Othman, M. E. Ya'acob, and M. Ahmadipour, "Parameter Extraction of Single, Double, and Three Diodes Photovoltaic Model Based on Guaranteed Convergence Arithmetic Optimization Algorithm and Modified Third Order Newton Raphson Methods," *Renew. Sust. Energy Rev.*, vol. 162, 2022. Doi: [10.1016/j.rser.2022.112436](https://doi.org/10.1016/j.rser.2022.112436)
 - [13] K. Chennoufi, M. Ferfra, and M. Mokhlis, "An Accurate Modelling of PV Modules Based on Two-Diode Model," *Renew. Energy*, 2020. Doi: [10.1016/j.renene.2020.11.085](https://doi.org/10.1016/j.renene.2020.11.085)
 - [14] M. Zaimi, H. El-Achouby, O. Zegoudi, A. Ibral, and E. M. Assaid, "New Analytical Approach for Modeling Effects of Temperature and Irradiance on Physical Parameters of Photovoltaic Solar Module," *Energy Convers. Manag.*, vol. 177, pp. 258-271, 2020. Doi: [10.1016/j.enconman.2018.09.054](https://doi.org/10.1016/j.enconman.2018.09.054)
 - [15] V. J. Chin, Z. Salam and K. Ishaque, "An Accurate and Fast Computational Algorithm for the Two-diode Model of PV Module Based on a Hybrid Method," in *IEEE Transactions on Industrial Electronics*, vol. 64, no. 8, pp. 6212-6222, Aug. 2017. Doi: [10.1109/TIE.2017.2682023](https://doi.org/10.1109/TIE.2017.2682023)
 - [16] PVsyst, "PVsyst Photovoltaic Software," [Online]. Available: <https://www.pvsyst.com/>.
 - [17] SolarPro, "SolarPro Simulation Software for PV Design," [Online]. Available: <https://www.solarpro.com/>.
 - [18] Solutions, I. P. V. (2019). 36 Cells - VE136PV. 10-11.
 - [19] Solar, T. (n.d.). The Honey Module (pp. 1-2).
 - [20] Hyundai. (2013). Hyundai Solar Module. 0-1. www.hyundaisolar.com

BIOGRAPHIES

Matheus Meireles da Silva was born in Caçador, Santa Catarina, Brazil, in 2002. He is currently pursuing a B.S. degree in Electrical Engineering at Federal University of Santa Catarina (UFSC). From July 2021 to April 2023, he was a member of the Electrical Engineering Tutorial Education Program of UFSC (PET EEL), where he held various coordination positions. He conducted voluntary scientific research at the Power Electronics Institute of UFSC (INEP) from July 2022 to November 2023, developing an application focused on quantizing electrical quantities in photovoltaic energy generation. From August 2023 to August 2024, he worked as an intern at the company ESSS, where he was able to work in the field of computational simulation applied to electromagnetism. Matheus has experience in computational simulation, electromagnetism, power electronics, and programming. He aims to further his studies and research, aspiring to make significant contributions to the field of Electrical Engineering.

Thiago Fonseca Rech received his B.E and M.E degrees in Electrical Engineering at the Federal University of Santa Catarina (UFSC) in 2019 and 2021. Currently, is pursuing a PhD degree at the Power Electronics Institute (UFSC) in Florianópolis, Brazil. His main research interests are modelling and simulation of power electronics systems, green hydrogen generation, optimization theory and renewable energy.

Tailan Orlando was born in Campinas do Sul, RS, Brazil, in 1996. He received the B.S. degree in electrical engineering in 2019 from the Integrated Regional University of Alto Uruguai and Missions (URI), Erechim, Brazil, and the M.S. degree in electrical engineering, in 2022, from the Federal University of Santa Catarina (UFSC), where he is currently working toward the Ph.D. degree at the Power Electronics Institute. His research interests include power converters, grid-connected systems, active filters, and green hydrogen generation. Ms. Orlando is member of the IEEE.

Victor Ferreira Gruner was born in Florianópolis, SC, Brazil. Graduated in Electrical Engineering, with an M.Sc. and Ph.D. in Power Electronics and Electric Drives. The professional career spans various R&D projects in the fields of energy processing, storage, and electric mobility. Throughout this journey, roles in R&D and Operations Management have provided valuable leadership opportunities, coordinating company activities and managing projects. With over a decade of experience in the field, a broad understanding of the industry has been developed. His main research interests in power electronics are grid connected inverters, SST applications and smart grid control.

Jens Friebe received the B.Sc., M.Sc., and Dr.-Ing. degrees in electrical engineering from the University of Kassel, Kassel, Germany. He was responsible for the research area of passive components in power electronics with the Institute for Drive Systems and Power Electronics, Leibniz University Hannover, Hanover, Germany, from 2018 to 2022. Before that, he was with SMA Solar Technology, Germany, in the field of PV-inverter topologies, wide-bandgap semiconductors, magnetic components, control strategies for high switching frequencies, and power electronics packaging, for more than 13 years. He is currently the Head of the Power Electronics Group, University of Kassel.

Kevin Rabelo Costa Graduated in Electrical Engineering from the Federal University of Ceará, Brazil, in 2019. In 2021, he completed a master's degree in electrical engineering, with an emphasis on Power Electronics and Embedded Systems, at the same university. Since 2022, has been working as an Assistant Researcher in the Power Electronics Department (LE-KDEE) at the University of Kassel, Germany, where he is also pursuing a Ph.D. His research focuses on the design and integration of power converters, magnetics, embedded control, and digital systems.

André Luís Kirsten was born in Santa Maria, Brazil, in 1986. He received the B.S., M.Sc., and Ph.D. degrees in electrical engineering from the Federal University of Santa Maria, Santa Maria, Brazil, in 2009, 2011, and 2014, respectively. He is currently a Professor with the Department of Electrical and Electronics Engineering at the Federal University of Santa Catarina (UFSC), Florianópolis, Brazil. His main research interests are power electronics, digital control, dual active bridge converter and solid-state transformers. Dr. Kirsten is member of SOBRAEP and IEEE.

Roberto Francisco Coelho received his B.Sc. degree in Electrical Engineering in 2006, his M.Sc. degree in 2007, and his Ph.D. degree in 2013, all from the Federal University of Santa Catarina (UFSC), Brazil. From March to August 2013, he was a researcher at the Center for Sustainable Energy (CES) of the CERTI Foundation. He is currently a permanent professor in the Graduate Program in Electrical Engineering (PPGEEL) at UFSC and serves as the Coordinator of the Undergraduate Course in Electrical Engineering at the same institution. He is also a member of the Board of the Brazilian Power Electronics Society (SOBRAEP), Associate Editor of the *Revista Eletrônica de Potência*, and Associate Editor of the Special Section "Energy Storage" of *Frontiers in Energy Research*. He has been regularly involved in research projects funded by development agencies and in collaboration with industry, and he is currently the coordinator of an international cooperation project between Brazil and Germany (PROBRAL/CAPES), running until 2027. His research interests include power converters, control, maximum power point tracker systems, grid-connected systems, and distributed generated systems. Dr. Coelho is member of the SOBRAEP and IEEE.